The Electron Dynamics of Shocked Polyethylene Crystal

Patrick L. Theofanis,[†] Andres Jaramillo-Botero,[*,†] Thomas R. Mattsson,[‡] Aidan P. Thompson,[‡] and William A. Goddard, III[*,†]

Division of Chemistry and Chemical Engineering, California Institute of Technology, 1200 E. California Blvd., Pasadena, CA 91125, USA, and Sandia National Laboratories, Albuquerque, NM 87185, USA

E-mail: ajaramil@caltech.edu; wag@wag.caltech.edu

Abstract

Electron force field (eFF) wavepacket molecular dynamics simulations of the single shock Hugoniot are reported for a crystalline polyethylene (PE) model. The eFF results are in good agreement with previous DFT theories and experimental data which is available up to 80 GPa. We predict shock Hugoniots for PE up to 350 GPa. In addition, we analyze the phase transformations that occur due to heating. Our analysis includes ionization fraction, molecular decomposition, and electrical conductivity during isotropic compression. We find that above a compression of 2.4 g/cm^3 the PE structure transforms into a Lennard-Jones fluid, leading to a sharp increase in electron ionization and a significant increase in system conductivity. eFF accurately reproduces shock pressures and temperatures for PE along the single shock Hugoniot.

Manuscript

The material response of polyethylene (PE) to shock and its behavior in the warm dense matter (WDM) regime is important because it is a common ablator material in direct-drive inertial confinement fusion (ICF) experiments.[1,2] Experiments at the National Ignition Facility (NIF) have demonstrated that the capsule material can have a considerable impact on the ICF burn efficiency.[2,3] Macroscopic modeling of capsule materials for these experiments requires accurate constitutive engineering models. Producing quality engineering models requires a detailed microscopic understanding of the equations of state (EOS), electrical conductivity, and optical properties for a given material. Here, we examine the effects of electronic excitations during hydrostatic shock of PE.

Theoretical studies of PE in extreme conditions are abundant. A variety of methods including quantum mechanics (QM), conventional forcefields, and reactive forcefields are able to reproduce a common equation of state gauge: the experimental Rankine-Hugoniot curve.[1,4] Born-Oppenheimer quantum molecular dynamics (BO-QMD) methods and conventional forcefields presume adiabaticity in their approach to simulating the high energy states of PE. This assumption limits the scope of these techniques to temperatures well below the Fermi-temperature, near the electronic ground state of PE.[5] Conventional and reactive forcefields are parameterized based on Born-Oppenheimer potential energy surfaces. The result of using Born-Oppenheimer methods is that the effects of electronic excitations are absent from the system's EOS, and along the particular EOS path corresponding to the Rankine-Hugoniot. Quantum mechanical finite-temperature density func-

*To whom correspondence should be addressed

[†]California Institute of Technology

[‡]Sandia National Laboratories, Albuquerque, NM 87185, USA

tional theory (DFT) methods, unlike BOQMD approaches, allow for electron excitations, however the Kohn-Sham orbital description precludes these methods from revealing dynamic electron effects like Auger processes.[6,7] Finite-temperature DFT methods, like those used in[4] and,[1] are good points of comparison because they allow for thermal electron excitations.

The first-principles-based electron forcefield (eFF) is a mixed quantum-classical approach for studying nonadiabatic reactive dynamics based on floating spherical Gaussian wavepackets.[8] In the past, eFF was successfully applied to nonadiabatic processes such as Auger decay,[9] H_2 in the WDM regime,[10] the hydrostatic[11] and dynamic[12] shock Hugoniot, and exo-electron emission due to fracture in silicon.[13] eFF is unique in that electronic and nuclear degrees of freedom are separate and this allows for non-adiabatic motion to occur naturally. eFF is also faster than QM, and this allows us to perform large scale and long-time-scale dynamics simulations.[12]

The eFF method provides an approximate description of quantum dynamics by describing every electron as a floating spherical Gaussian orbital whose position and size varies dynamically while the nuclei are treated as classical point charge particles.[14] Here the total N-electron wavefunction is written as a Hartree product of one-electron orbitals (rather than as an antisymmetrized product). Orthogonality resulting from the Pauli Principle is enforced with a spin-dependent Pauli repulsion Hamiltonian which is a function of the sizes and separations of these Gaussian orbitals. The Pauli potential accounts for the kinetic energy change due to orthogonalization, arising from the Pauli principle (antisymmetrization).[8,15] An additional quantum-derived term in the eFF Hamiltonian is the kinetic energy for each orbital, which accounts for the Heisenberg principle. The full Hamiltonian in eFF also incorporates classical electrostatic terms between nuclei or electrons. For this study we used a parallel version of eFF which is included in the LAMMPS software package[12,16]

A crystalline PE model was created by truncating and hydrogen passivating the chains in a $2 \times 6 \times 3$ supercell of orthorhombic polyethylene. Truncating the chains in this fashion prevents unnatural stresses from forming along the length of each chain. The final cell contained 12 $C_{12}H_{26}$ molecules: 1,632 particles total, 144 carbon, 312 hydrogen and 1,176 electrons. In real samples of crystalline PE the chains are finite in length and the PE is only crystalline in small domains with lamella ranging from 70 to 300 Å in thickness and extending several microns laterally.[17,18] Because eFF lacks van der Waals forces, the equilibrium volume of crystalline PE is 30% too large in eFF. To counter this, the volume of the PE cell was adjusted so that the ground state reference has a density of 0.95 g/cm^3; this produced 1.3 GPa of stress which was subtracted from all subsequent pressure computations. To generate points along the Hugoniot path, we prepared samples of increasing density up to 3.0 g/cm^3 by isothermally and isotropically compressing the reference cell at 300 K. Each cell was then ramped to 1,500 K over the course of 500 fs and it was allowed to equilibrate as an NVE ensemble at 1,500 K for another 500 fs. After heating each cell was cooled by decreasing the temperature in 30 K steps during which 200 fs of NVT dynamics was followed by 200 fs of NVE dynamics. The Nosé-Hoover thermostat was used for sample preparation.

In the eFF method the electron mass is defined in three separate locations: 1) in the electronic kinetic energy, (i.e. wavefunction); 2) in the spin-dependent Pauli energy; and 3) in the equations of motion.[8,12] The effect of modifying the electron mass in 1) and 2) affects the sizes of electrons in atoms and the lengths of bonds in molecules therefore we keep these fixed to avoid disrupting the chemistry of the system. In all potential energy terms the electron mass is set to the true electron mass (5.486×10^{-4} amu). The user may define a different *dynamic electron mass* to evolve the kinetic equations of motion.[8,12] Changing the mass in the equations of motion varies the overall time scale of excited electron motions, with the time scale of excitation relaxations and energy transfer proportional to $\sqrt{m_e}$. This is what we refer to as changing the dynamic masses. This does not affect the net partitioning of energy in the system nor the magnitude of the thermodynamic parameters we are interested in measuring. This does not alter the system's chemistry, just its evolution in time. We verified this by computing a few Hugoniot points with 1.0 amu, 0.1, and 0.01

amu electrons and found negligible differences in pressure and temperature at these points. An artificially heavy electron mass enables the use of longer integration time steps. For this study we set the dynamic electron mass to 0.1 amu. To conserve mass in the system we subtracted the mass of each atom's electrons from the standard atomic mass (e.g. we set carbon atom masses to 11.4107 amu and hydrogen atom masses to 0.90794 amu). Because we used light electrons we used an integration time step of 0.5 attoseconds (0.0005 fs).

The temperature in eFF (like pressure) is extracted from dynamics simulation using classical virial expressions summing the kinetic energies of all nuclear and electronic degrees of freedom:

$$E_{ke} = \frac{3}{2} N k_B T \tag{1}$$

The kinetic contribution to the heat capacity is set to $\frac{3}{2}k_B$ by setting N to the number of nuclei which is valid for temperatures well below the Fermi temperature. The temperatures presented in this manuscript were computed using Eq. (1).

A Hugoniot curve is the locus of thermodynamic states that can be reached by shock compression of an initial state. These states satisfy the Rankine-Hugoniot energy condition[19,20]

$$U - U_0 = \frac{1}{2}(P + P_0)(V_0 - V) \tag{2}$$

where U is the internal energy, P is the pressure of the system, and V is the cell volume. It is assumed that each point on this seam corresponds to a state of thermodynamic equilibrium wherein the stress state is hydrostatic. For solids, this latter condition is only valid when the yield stress is much lower than the mean stress.[21] When the initial state variables P_0, V_0, and U_0 are those of the uncompressed sample at room temperature, the Rankine-Hugoniot curve is called the principal Hugoniot. We generated states on the principal Hugoniot using the following iterative procedure. First the volume of the system is specified, representing a particular degree of compression. How each density point was prepared is described in the preceding paragraph. The temperature of the system is quickly increased by changing the set-point of the thermostat. 100 fs of dynamics are run after the thermostat jump, during which averages of the energy, temperature and pressure of the new state are obtained. These values are used to evaluate the residual energy E_{res}, given by

$$E_{res} = (U - U_0) - \frac{1}{2}(P + P_0)(V_0 - V). \tag{3}$$

When $E_{res,i}/E_{ke,i} < 0.05$ the Hugoniot condition is considered satisfied. If this inequality is not satisfied an additional 100 fs iteration is performed. The new thermostat setpoint is calculated from:

$$T_{i+1} = T_i \left(1 + 0.05 \frac{E_{res,i}}{E_{ke,i}} \right) \tag{4}$$

where $E_{ke,i}$ is the average kinetic energy of the system at step i. Once this iterative procedure has converged, the thermostat is turned off and the system is allowed to propagate as a microcanonical (NVE) ensemble for an additional 1 ps. This calculation ensures that the Hugoniot condition is actually met and the properties of the systems were obtained from these dynamics.

Figure 1 is the principal Hugoniot projected onto the pressure-density plane. For compressions below 2.0 g/cm^3 eFF matched the experimental and DFT Hugoniot points quite closely (see Figure 1b). At higher densities the eFF simulations overpredicted the shock pressure relative to DFT. Above 2.0 g/cm^3 the results show that eFF is systematically "stiffer" than the experimental and DFT/AM05[22] data. However, eFF outperforms several classical MD potentials such as AIREBO,[23] OPLS,[24] and exp-6 (not shown);[25] the data for these can be found in.[4] eFF also outperformed the tight-binding QM method above 2.0 g/cm^3. These results demonstrate the difficulty in modeling the behavior of materials under shock compression. Figure 2 shows the temperature-pressure plane of the Hugoniot calculated by the methods in Figure 1 for which temperature data was available. The system temperatures produced by the eFF calculations are in good agreement with conventional forcefields, reactive forcefields and QM.

At high compression interesting material features appear in the principal Hugoniot. In the AM05 data series a shoulder feature appears at 2.3 g/cm^3. This feature is not as pronounced in

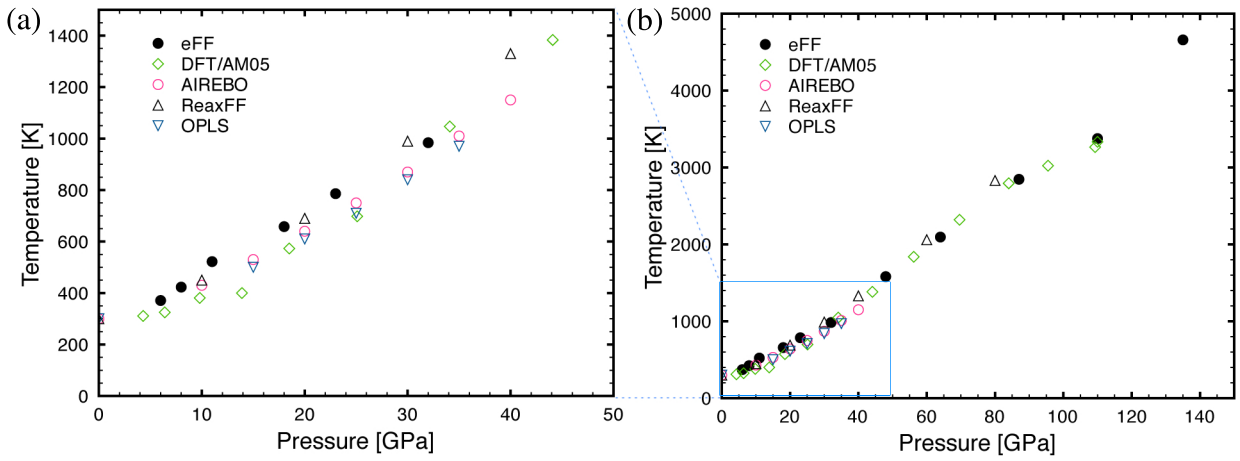

Figure 2: (a) The pressure-temperature locus of the Hugoniot curve for the eFF, DFT/AM05, OPLS, AIREBO and ReaxFF methods. (b) The pressure-temperature seam at greater pressures.

the eFF Hugoniot, however, for both methods inflections in the temperature-density plane of the Hugoniot curve indicate phase transitions (see Figure 3). Subtle temperature suppression is evident in the eFF temperature-density curve at 2.0 and 2.6 g/cm^3. These data features correspond to tangible transitions in the the molecular structure. Mattsson reported that the AM05 shoulder at 2.3 g/cm^3 corresponded to PE backbone bond breaking.[4] The causes for the eFF data features will be discussed shortly.

An analysis of the pairwise radial distribution functions (RDFs) for different degrees of compression demonstrates that significant structural decomposition occurs upon shock. Figure 4(a) shows that carbon bonds are compressed as the sample is compressed. As the density of the material increases the nearest neighbor C-C pair peak (1.55 Å) broadens and the next nearest neighbor C-C pair distance (2.6 Å) is lost indicating that the carbon backbone is fragmented. The C-H pair distribution function in Figure 4b indicates a gradual phase change to an atomic fluid of hydrogens. The 2.9 g/cm^3 series resembles a Lennard-Jones fluid. At this level of shock compression the hydrogen are totally dissociated from the PE chains. The H-H pair distribution function in Figure 4c also shows that order is lost. At high compression the H-H RDF also resembles a Lennard Jones fluid. From this data we conclude that the structure is shocked strongly enough to cause a phase transition to a state where the carbon backbones remain partially intact but they are solvated by loosely associated hydrogen atoms. For densities corresponding to temperatures around 3,000 K small peaks in the H-H data in Figure 4c near 0.7 shows that molecular hydrogen is formed. Mattsson and collaborators also found hydrogen formation when their shocked PE reached 2,800-3,100 K.[29] In their simulations and in the eFF simulations this temperature range corresponded to densities of 2.2-2.3 g/cm^3. For temperatures higher than 3,100 K the molecular hydrogen becomes too energetic to stay bound, and at lower temperatures the hydrogen do not have enough energy to dissociate from their polyethylene backbone. The eFF results are consistent with MD and DFT results for equivalent temperatures.

One of eFF's greatest assets is its ability to separate electron degrees of freedom, energies, positions, momentum, and forces from those of the nuclei. This gives us unrivaled ability to measure electronic physical quantities. In our investigation of PE we have used this to measure the ion fraction at each stage of shock. To do this we measure the kinetic and potential energy of each electron at each timestep in our simulations. Figure 5 shows the onset of electron ionization at 2.5 g/cm^3. Ionization increases exponentially. The rapid increase in ionization fraction above 2.6 g/cm^3 is evidently the cause of the shoulder in the temperature-density Hugoniot between 2.6 and 2.7 g/cm^3. Above this threshold electron ionization draws energy from the system and this af-

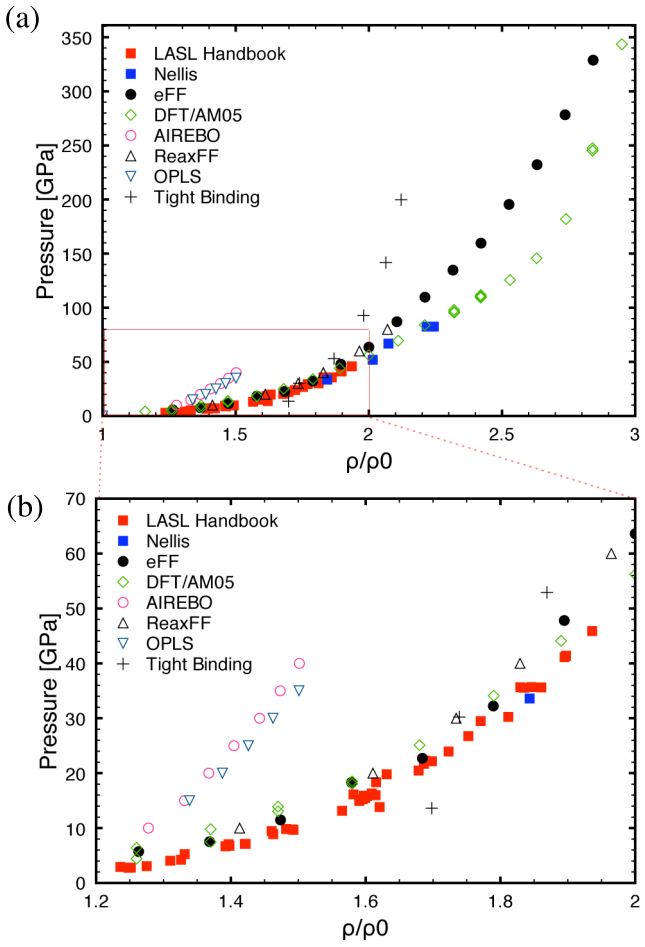

Figure 1: (a) The principal Rankine-Hugoniot for PE. Experimental data from the LASL shock compression handbook[26] and Nellis[27] is provided along with data for the classical MD potentials, OPLS,[4] and AIREBO,[4] a reactive force field, ReaxFF,[4] and quantum mechanical approaches, DFT/AM05 and tight binding,[28] are included for comparison. (b) An expansion of the low compression region of the Hugoniot.

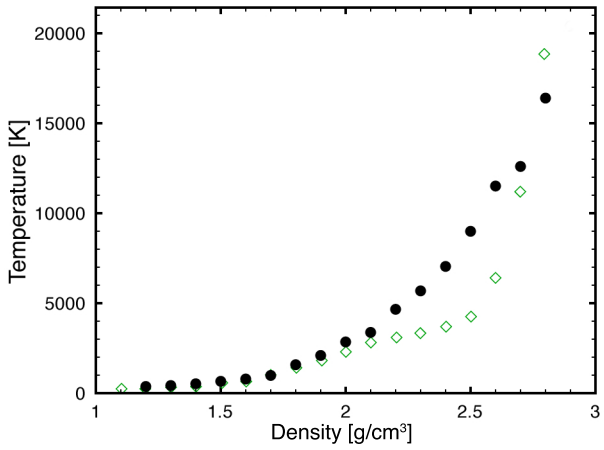

Figure 3: The temperature-density plane of the principal Hugoniot for the eFF (black circles) and DFT/AM05 (open green diamonds) methods.

fects the pressure and temperature of the Hugoniot. The production of carriers in our simulations implies that PE is conductive at high states of compression. The production of ions is precipitated by the breaking of C-C bonds, and this relationship is evident in Figure 5. The percentage of intact backbone for the DFT/AM05 study is also presented in Figure 5. eFF predicts that the polymer backbone begins to fracture at 2.4 g/cm^3 and DFT/AM05 predicts that fracture begins at 2.0 g/cm^3. This discrepancy is due to the fact that eFF overestimates the strength of carbon-carbon σ-bonds (for ethane the bond dissociation energy is 140 kcal/mol versus 90 kcal/mol experimental).[8]

In order to quantify the conductivity of the shocked system we determined the direct current conductivity using a classical Green-Kubo analysis.[30,31] We determined the electrical conductivity from our NVE Hugoniot states using the Green-Kubo integral of the electric current correlation function:

$$\sigma_{GK} = \frac{1}{3k_BTV}\int_0^\infty \left\langle \mathbf{j}(t)\cdot\mathbf{j}(0)\right\rangle \mathrm{d}t \qquad (5)$$

where $\mathbf{j}(t)$ is the electric current flux, and the integral argument corresponds to the electric current velocity correlation that is expressed as,

$$J(t) = \left\langle \mathbf{j}(t)\cdot\mathbf{j}(0)\right\rangle = \sum_{i=1}^{N}\sum_{j=1}^{N}\left\langle q_iq_j\mathbf{v}_i(t)\cdot\mathbf{v}_j(0)\right\rangle \qquad (6)$$

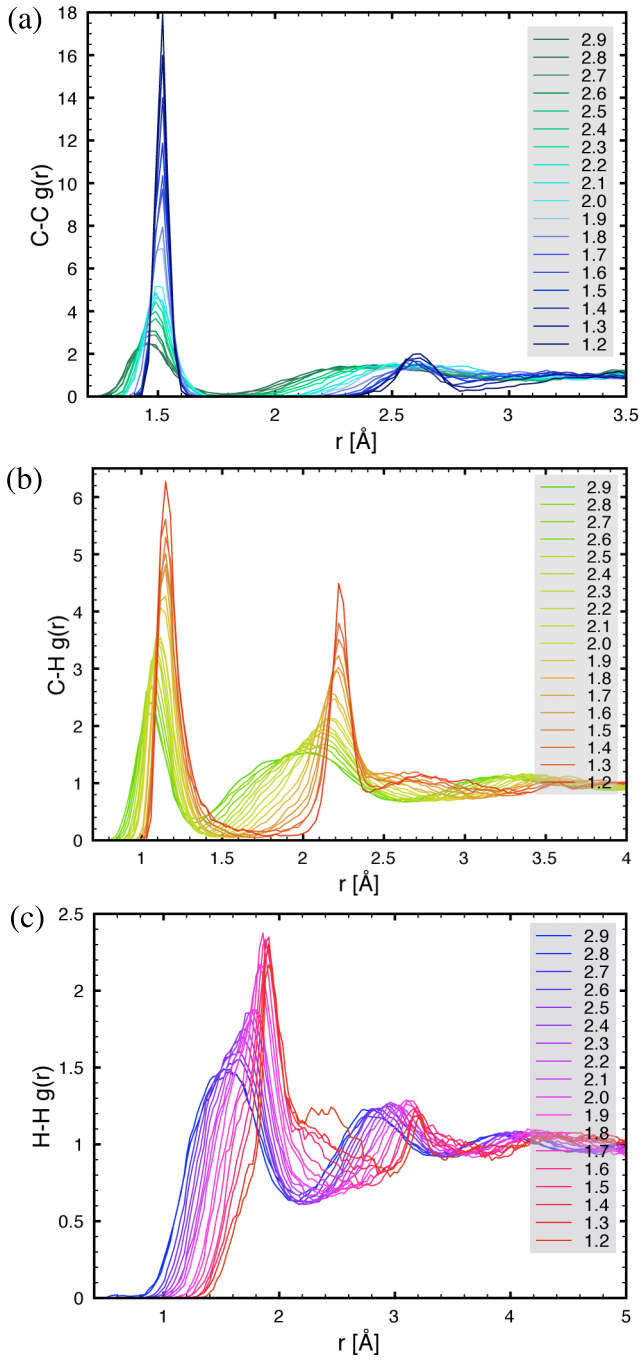

Figure 4: Radial distribution functions for (a) C-C atom pairs, (b) C-H pairs, and (c) H-H pairs.

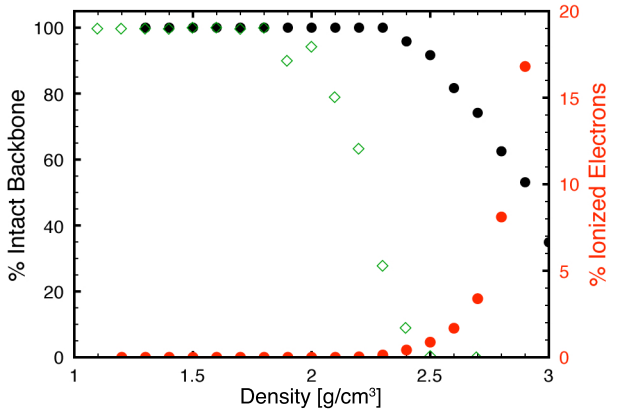

Figure 5: Structural decomposition along the PE Hugoniot. The open black circles and open green diamonds correspond to the % intact C-C backbone for the eFF and DFT/AM05 simulations, respectively. The red circles are the average % ionization along the Hugoniot calculated from the eFF simulations.

where i and j are different particles, q is the charge on each particle, $\mathbf{v}(t)$ is the velocity of each particle. Figure 6 shows the results of this analysis for eFF Hugoniot points. eFF predicts that conductivity increases exponentially along the Hugoniot curve. At 2.9 g/cm^3 the sample has a conductivity of 2.1 S/cm which is roughly equivalent to the conductivity of germanium, for example. Indeed, quantum mechanical studies of PE in the warm dense matter regime find conductivities between 0.3×10^4 and 1×10^4 S/cm for samples at 1 g/cm^3 and 11,605 K to 3 g/cm^3 and 34,815 K.[1]

We have simulated the response of PE to hydrostatic shock compression using the eFF wavepacket molecular dynamics method. eFF accurately reproduces previously published experimental and theoretical findings for high energy shock Hugoniots of PE and provides further insight into the effects of electron excitations and ionization at extreme pressures and temperatures (e.g. above 2.4 g/cm^3 the polymer backbone begins to break and electrons exponentially ionize). For 300 GPa shocks significant structural deterioration and ionization will occur. eFF also enabled us to study the electronic conductivity of PE as it transitions at high temperatures into a plasma phase; a unique features that is impossible to obtain via conventional force fields or QM. The fi-

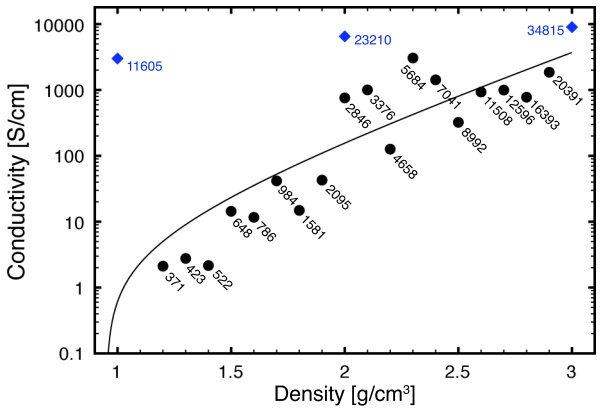

Figure 6: The direct current electrical conductivity of points along the eFF Hugoniot curve (black circles) and finite temperature DFT (blue diamonds) from Horner 2010.[1] Temperatures for each data point are provided.

delity of the eFF Hugoniot indicates that van der Waals interactions are not important under shock conditions. We expect the results presented in this paper will stimulate further work on the applicability of eFF to open problems in high energy-density physics.

Acknowledgement

Patrick Theofanis would like to thank John Aidun, Aidan Thompson, and Thomas Mattsson for hosting him at Sandia National Laboratories, where part of this work was initiated. This Material is based upon work supported by the Department of Energy National Nuclear Security Administration under Award Number DE-FC52-08NA28613.

Sandia National Laboratories is a multiprogram laboratory managed and operated by Sandia Corporation, a wholly owned subsidiary of Lockheed Martin Corporation, for the U.S. Department of Energy's National Nuclear Security Administration under Contract No. DE-AC04-94AL85000.

References

(1) Horner, D. A.; Kress, J. D.; Collins, L. A. Effects of metal impurities on the optical properties of polyethylene in the warm dense-matter regime. *Phys. Rev. B* **2010**, *81*, 214301.

(2) Sangster, T. C. et al. Cryogenic DT and D2 targets for inertial confinement fusion. *Phys. Plasmas* **2007**, *14*, 058101.

(3) Amendt, P.; Cerjan, C.; Hamza, A.; Hinkel, D. E.; Milovich, J. L.; Robey, H. F. Assessing the prospects for achieving double-shell ignition on the National Ignition Facility using vacuum hohlraums. *Phys. Plasmas* **2007**, *14*, 056312.

(4) Mattsson, T. R.; Lane, M. D.; Cochrane, K. R.; Desjarlais, M. P.; Thompson, A. P.; Grest., G. P. First-principles and Classical Molecular Dynamics Simulation of Shocked Polymers. *Phys. Rev. B.* **2010**, *81*, 054103.

(5) Pittalis, S.; Proetto, C. R.; Floris, A.; Sanna, A.; Bersier, C.; Burke, K.; Gross, E. K. U. Exact Conditions in Finite-Temperature Density-Functional Theory. *Phys. Rev. Lett.* **2011**, *107*, 163001.

(6) Mermin, N. D. Thermal Properties of the Inhomogeneous Electron Gas. *Phys. Rev.* **1965**, *137*, A1441–A1443.

(7) Car, R.; Parrinello, M. Unified Approach for Molecular Dynamics and Density-Functional Theory. *Phys. Rev. Lett.* **1985**, *55*, 2471–2474.

(8) Su, J. T. An Electron Force Field for Simulating Large Scale Excited Electron Dynamics. Ph.D. thesis, California Institute of Technology., Pasadena, CA, 2007.

(9) Su, J. T.; Goddard III, W. Mechanisms of Auger-Induced Chemistry Derived from Wave Packet Dynamics. *Proc. Nat. Acad. Sci.* **2009**, *106(4)*, 1001–1005.

(10) Su, J. T.; Goddard III, W. A. Excited Electron Dynamics Modeling of Warm Dense Matter. *Phys. Rev. Lett.* **2007**, *99*, 185003.

(11) Kim, H.; Su, J. T.; Goddard III, W. A. High-temperature high-pressure phases of lithium from electron force field (eFF) quantum electron dynamics simulations. *Proc. Nat. Acad. Sci.* **2011**, *108*, 15101–15105.

(12) Jaramillo-Botero, A.; Su, J. T.; Qi, A.; Goddard III, W. A. Large-Scale, Long-Term Nonadiabatic Electron Molecular Dynamics for Describing Material Properties and Phenomena in Extreme Environments. *J. Comp. Chem.* **2010**, *32*, 497–512.

(13) Theofanis, P. L.; Jaramillo-Botero, A.; Goddard III, W. A.; Xiao, H. Non-Adiabatic Study of Electron Effects During Brittle Fracture in Silicon. *Phys. Rev. Lett.* **2011**, *in review*.

(14) Frost, A. A. Floating Spherical Gaussian Orbital Model of Molecular Structure. I. Computational Procedure. LiH as an Example. *J. Chem. Phys.* **1967**, *47*, 3707–3713.

(15) Wilson, C. W.; Goddard III, W. A. Exchange Kinetic Energy, Contragradience, and Chemical Binding. *Chem. Phys. Lett.* **1970**, *5(1)*, 45–49.

(16) Plimpton, S. J. Fast Parallel Algorithms for Short-Range Molecular Dynamics. *J. Comp. Phys.* **1995**, *117*, 1–19.

(17) Doyle, M. J. *Polym. Eng. Sci.* **2000**, *40(2)*, 330–335.

(18) Bourne, N. K.; Millett, J. C. F.; Goveas, S. G. The shock response of polyoxymethylene and polyethylene. *J. Phys. D.: Appl. Phys.* **2007**, *40*, 5714–5718.

(19) Rankine, W. J. M. *Phil. Trans. Roy. Soc.* **1870**, *160*, 277.

(20) Hugoniot, H. *J. de l'Ecole Polytechnique* **1887**, *57*, 3.

(21) Boslough, M. B.; Asay, J. R. *High-Pressure Shock Compression of Solids, ed. by JR Asay and M Shahinpoor.*; Springer-Verlag: New York, NY, 1993; p 7.

(22) Armiento, R.; Mattsson, A. E. Functional Designed to Include Surface Effects in Self-Consistent Density Functional Theory. *Phys. Rev. B* **2005**, *72*, 085108.

(23) Stuart, S. J.; Tutein, A. B.; Harrison, J. A. A Reactive Potential for Hydrocarbons with Intermolecular Interactions. *J. Chem. Phys.* **2000**, *112*, 6472.

(24) Jorgensen, W. L.; Maxwell, D. S.; Tirado-Rives, J. Development and Testing of the OPLS All-Atom Force Field on Conformational Energetics and Properties of Organic Liquids. *J. Am. Chem. Soc.* **1996**, *118*, 11225.

(25) Borodin, O.; Smith, G. D.; Bedrov, D. Development of Many-Body Polarizeable Force Fields for Li-Battery Components: 1. Ether, Alkane, and Carbonate-Based Solvents. *J. Phys. Chem. B.* **2006**, *110*, 6279.

(26) *LASL Shock Handbook, edited by S.P. March*; University of California Press: Berkeley, CA, 1980.

(27) Nellis, W.; Ree, F.; Trainor, R.; Mitchell, A.; Boslough, M. Equation of State and Optical Luminocity of Benzene, Polybutene, and Polyethylene Shocked to 210 GPa. *J. Chem. Phys.* **1984**, *80*, 2789.

(28) Kress, J. D.; Bickham, S. R.; Collins, L. A.; Holian, B. L.; Goedecker, S. Tight-binding molecular dynamics of shock waves in hydrocarbons. *AIP Conference Proceedings* **2000**, *505*, 381–384.

(29) Mattsson, T. R.; Cochrane, K. R. Private communication.

(30) Shim, Y.; Kim, H. J. *J. Phys. Chem. B* **2008**, *112*, 11028–11038.

(31) Kowsari, M. H.; Alavi, S.; Najafi, B.; Gholizadeh, K.; Dehghanpisheh, E.; Ranjbar, F. Molecular dynamics simulations of the structure and transport properties of tetrabutylphosphonium amino acid ionic liquids. *Phys. Chem. Chem. Phys.* **2011**, *13*, 8826–8837.